Part I

Feedback-free fluidic oscillators based on impinging jets

Introduction

Fluidic oscillators are devices that issue an oscillating jet of fluid when supplied with a continuous stream of pressurized gas or liquid; as such, they can be seen as fluidic DC/AC converters. They started to be studied in the 1960s, as well as other fluidic devices functioning with no moving parts, such as fluidic logic elements or fluidic amplifiers (Angrist, 1964; Glaettli, 1964; Tanney, 1970). There are two main types of fluidic oscillators: wall-attachment devices and jet-interaction devices (see figure I.1). The wall-attachment oscillators are based on the Coandă effect, where the fluid jet interacts with an adjacent wall, which results in its deflection. The jet-interaction devices also named "feedback-free" devices are based on the interactions of two jets inside an interaction chamber having a specific geometry (Raghu, 2001).

Only a few industrial applications of fluidic oscillators have emerged over the years, such as flow metering (Beale and Lawler, 1974) and windshield washer devices (Stouffer, 1985), however, with the development of microfluidics and its applications to lab-on-chip devices, a renewed interest for fluidic devices appeared, and in particular for fluidic devices with no moving parts, such as static micromixers (Bertsch et al., 2001) or fluidic diodes (Anduze et al., 2001; Fani et al., 2013; Haward et al., 2016).

Most research work performed so far on microfluidic oscillators operating with liquids aims either at the study of new types of static micromixers or at the implementation of fluidic logic circuits. A small number of such fluidic oscillators have been described in the scientific literature, and implement a variety of working principles.

Notwithstanding active microfluidic oscillators have been studied (Niu and Lee, 2003), here we mainly focus on passive oscillators, where a constant liquid flow is applied at the inlets and oscillations are generated by the design of the microfluidic network. One of the most studied types of microfluidic oscillators is based on the use of fluidic resistors, capacitors and valves, and uses the analogy between the electrical and fluidic domains, where voltage is replaced by pressure and electrical current is replaced by hydraulic volume flow. The microfluidic equivalents of electrical resistors are channels, microfluidic capacitors are chambers with membranes that store energy by membrane deformation, while equivalents of diodes, and transistors, are valves of diverse designs that can completely shut off the flow in given conditions. Based on this electronic-fluidic analogy, a fluidic astable multivibrator driven by a constant pressure flow was described by Lammerink et al. (1995). This concept was further developed later, taking advantage of the versatility of the microfabrication methods based on the use of polydimethylsiloxane (PDMS), an elastomeric material that renders the fabrication

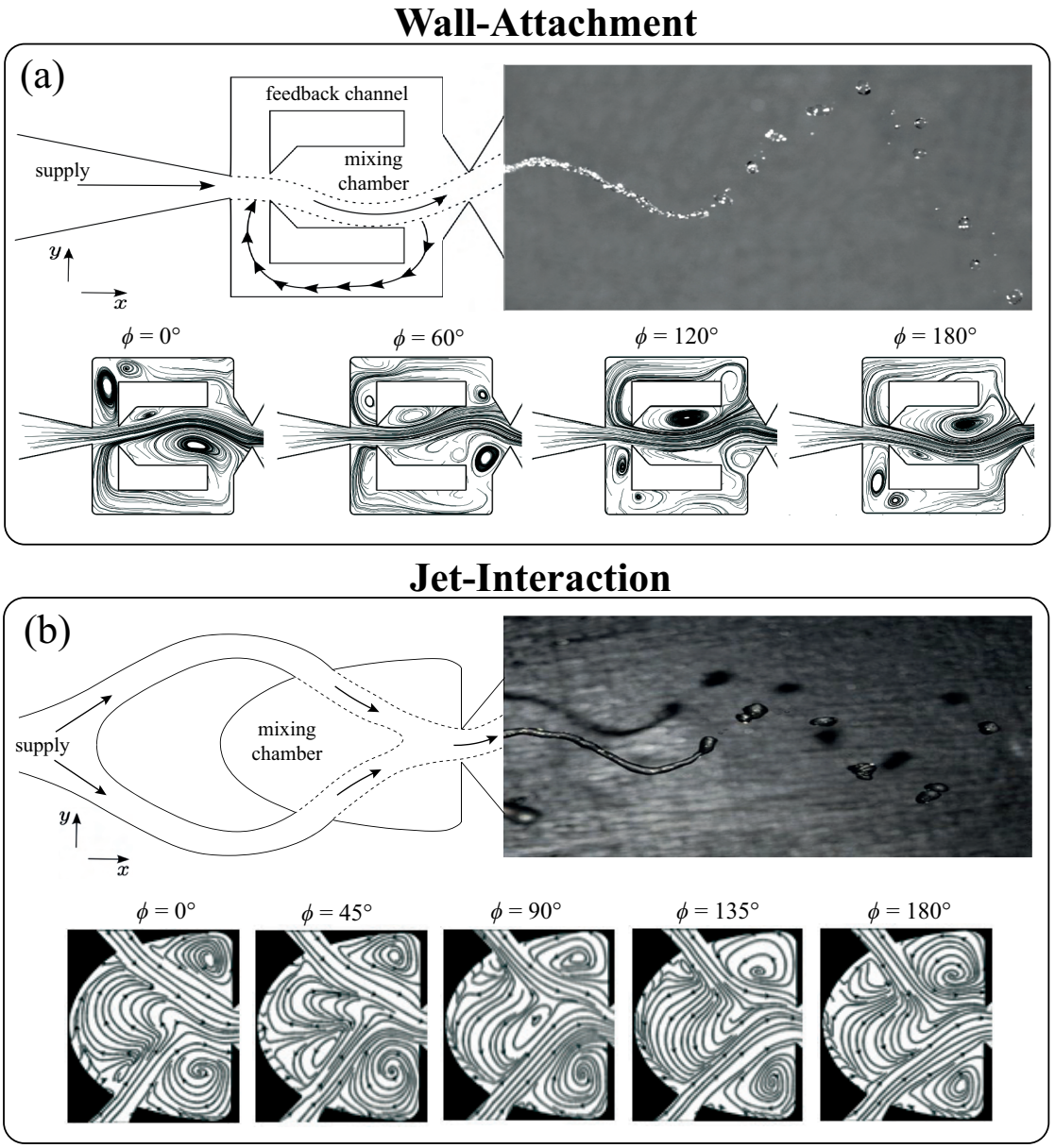

Figure I.1 – (a) A fluidic oscillator based on wall-attachment. The feedback mechanism is provided by two feedback channels. Four snapshots of the first half of the oscillation cycle are shown: φ denote the corresponding flow phase-angle. Visualization as streamlines numerically computed (modified figure from Woszidlo et al. (2015)). (b) A fluidic oscillator based on two jets interacting within a mixing chamber. Four snapshots of the first half of the oscillation cycle are shown as streamlines numerically computed (modified figure from Tomac and Gregory (2014)).

of fluidic networks containing membranes very simple. Mosadegh et al. (2010) demonstrated a microfluidic oscillator and used it to perform flow-switching and clocking functions. Kim et al. (2011, 2013) fabricated a number of devices based on this type of microfluidic oscillator,

among which a micromixer and an autonomous pulsed flow generation system capable of generating on-demand and independently a range of flow rates and a range of flow oscillation frequencies (Li and Kim, 2017). (Kim et al., 2015) applied it in studying endothelial cell elongation response to fluidic flow patterns. Devaraju and Unger (2012) also demonstrated a fluidic oscillator, among many other fluidic logic functions and Nguyen et al. (2012) performed peristaltic pumping on chip using a control signal generated on chip through a fluidic oscillator circuit.

Xia et al. (2012) also developed a micromixer based on a vibrating elastomeric diaphragm trapped in a two-level cavity. Here, there is no need for a complex fluidic circuit as the deformation of the diaphragm directly creates the oscillating liquid flow, but the wear of the elastomeric material limited the use of this device. Simpler microfluidic oscillators containing no moving parts, no deformable membranes and no complex fluidic circuit have also been studied by several authors. These oscillators are based on jets interacting in a simple cavity and generating an oscillating flow (Gregory et al., 2007; Tomac and Gregory, 2012). Yang et al. (2007) demonstrated that feedback-driven microfluidic oscillators based on the Coandă effect can generate an oscillatory liquid flow at small Reynolds numbers. Their design used a micro-nozzle with a sudden expansion and asymmetric feedback channels and measured oscillatory frequencies of the flow below 1 Hz for Reynolds numbers between 1 and 100. Similar oscillator designs were later studied experimentally by Xu and Chu (2015) to develop feedback micromixers based on the Coandă effect. They demonstrated that there were three different oscillating mechanisms that resulted in mixing in such structures, depending on the magnitude of the Reynolds number: vortex mixing, internal recirculation mixing, and oscillation mixing. Xie and Xu (2017) simulated the fluidic behaviour of such devices using the Fluent® CFD software.

Finally, Sun et al. (2017); Sun and Sun (2011) studied liquid mixing resulting from a microfluidic oscillator using an impinging jet on a concave semi-circular surface. This type of microfluidic oscillator is another example of the use of the Coandă effect. Oscillations were observed for Reynolds numbers as low as 70, with the frequency of oscillations below 1 Hz.

In **Chapter 2**, we present a microfluidic oscillator that can be classified in the jet-interaction device category. It has a very simple configuration, i.e. X-shaped cross-junction where two incoming streams meet head-to-head and exhaust into two outlet channels (see figure I.2). Its oscillations depend on the jet interactions more than on the shape of the surrounding cavity. This device is based on facing impinging liquid jets and operates in laminar flow conditions. Observations of flow patterns obtained with micromixers having geometries similar to the ones presented in this paper but much larger dimensions were performed by Tesař (2009), however, the manufacturing method of these devices limited their aspect ratios and allowed to perform observations of only a limited part of the phenomenon. Impinging self-oscillating jets have been described in scientific literature by Denshchikov et al. (1978) using facing turbulent water jets, having dimensions in the centimeter range immersed in a 230L water tank. In a follow-up paper (Denshchikov et al., 1983), the period of the auto-oscillating phenomenon

was empirically described by a set of equations. If the phenomena described in this work show some similarities with the jet configuration presented in (Denshchikov et al., 1978, 1983), the jets dimensions are orders of magnitude smaller and the flow conditions remain laminar (Lashgari et al., 2014).

We provide a detailed experimental and numerical description of the self-sustained oscillatory regime and we study the evolution of the self–oscillation frequency when the main geometric parameters of the cavity are changed. Most interestingly, the shedding frequency is shown to be proportional to the averaged flow velocity imposed at the symmetric inlets and inversely proportional to the distance between the jets, irrespective of many other parameters, such as channel width, depth, length, Reynolds number, etc.

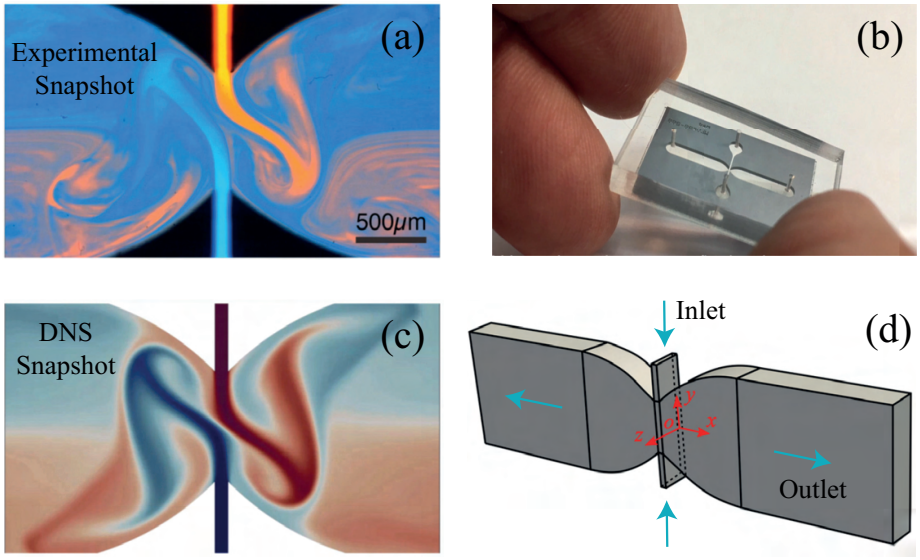

Figure I.2– (a) Snapshot of the self-sustained oscillatory flow obtained experimentally and (c) numerically (via DNS) in our flaring X-junction (*Center*) for a Reynolds number greater than the critical one, Re_{cr}. See also https://doi.org/10.1103/APS.DFD.2019.GFM.V0036 for a Gallery of Fluid Motion award-winning video). The actual device is shown in (b), while an example of a computational domain for DNS is illustrated in (d).

By analogy with the cylinder flow discussed in Chapter 1, the oscillatory instability described in Chapter 2, is experimentally seen to be of supercritical nature with oscillations starting above a precise instability threshold, i.e. $Re > Re_{cr}$. Although several plausible candidates are proposed, at this stage no physical mechanism could be precisely identified from which the self-sustained oscillations would originate, thus calling for a significant interpretation effort.

Furthermore, cross-slot flows are also known to show hysteresis. For instance, Burshtein et al. (2019) experimentally showed that hysteretic behaviours due to symmetry-breaking transitions appear in X-junction flows with proper geometrical parameters, for which no oscillations are observed (see figure I.3). There are similarities in the microchannel geometries between the case described by Burshtein et al. (2019) and the one presented in this work, with microchannels crossing at right angle in both cases and liquid flows at relatively low values

of the Reynolds number. However, in the geometry considered by Burshtein et al. (2019) all channels have comparable dimensions, whereas here, there are two facing narrow channels which open into wider channels. Particularly, we observe oscillations only in the cases where the wider channels have dimensions at least 3 times larger than the narrow channels, which differs significantly from Burshtein et al. (2019). Such a consideration further underlines the importance of the distance separating the inlets in cross–slot geometries in the destabilization mechanism.

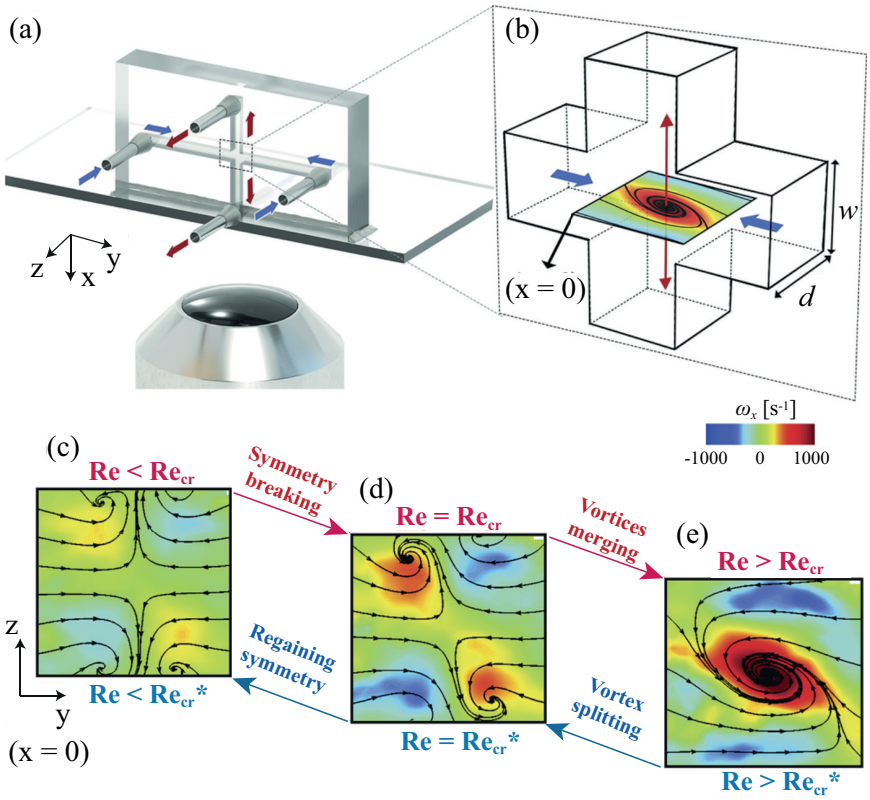

Figure I.3– Study of the vortex dynamics and interactions associated with a symmetry-breaking flow instability at a 4-way intersection (Burshtein et al., 2019). The merging and the splitting of vortices are connected with the symmetry-breaking transition and are affected by the degree of vortex confinement, i.e. by the geometry. (a) A schematic diagram of the experimental setup of Burshtein et al. (2019), which allows a direct observation of the $x = 0$ plane on an inverted microscope. Inflow (along y) is indicated by the blue arrows, and outflow (along x) is indicated by the red arrows. (b) Schematic diagram of a vortex in the cross-slot device for flow at $Re > Re_{cr}$; d and w are the channel depth and width, respectively. (c,e) μ-PIV images of the vorticity field at $x = 0$: (c) a symmetric flow field with four cells of Dean vortices; (d) an asymmetric flow field where two intensified Dean vortices have commenced merging; and (e) a single steady, central streamwise vortex is formed by the merging of the two Dean vortices.

Hence, **Chapter 3** aims at answering two main questions arising from different observations presented in Chapter 2 (Bertsch et al., 2020a,b) and by Burshtein et al. (2019): (i) to identify

the physical mechanism governing the self-sustained oscillatory regime studied in Bertsch et al. (2020a); (ii) to investigate the existence of a range of geometrical parameters in which steady symmetry-breaking conditions could directly interact with this dynamic instability.

With these objectives, we consider a two-dimensional (2D) X-junction with straight lateral channels and two symmetric inlets, where a fully developed flow is imposed, separated by a certain distance. Despite the simplistic geometry, a 2D flow not only allows one to perform a faster computational analysis but also often makes it possible to capture the main physical features of interest in the 3D problem. Particularly, since the main geometrical parameter, i.e. the distance between the two jets, is kept in this crude dimensional reduction from 3D to 2D, we may expect that our 2D analysis reveals the dominant physical mechanism behind the oscillatory instability observed in 3D. Steady symmetry-breaking instabilities are also expected in 2D (Liu et al., 2016; Pawlowski et al., 2006), even though their nature differs from the intrinsically 3D one presented in Burshtein et al. (2019). An exhaustive stability analysis is here conducted using the tools of the classic linear global stability and sensitivity analysis as well as the weakly nonlinear theory based on amplitude equations.

Precisely, global stability identifies a region of geometrical and flow parameters where two unstable global modes become simultaneously unstable. One of the modes is responsible for the self-oscillations, whereas the other induces a steady symmetry-breaking. The interaction of such modes is described by means of amplitude equations, whose resulting predictions are confirmed by DNS. The weakly nonlinear model also predicts an oscillation frequency that scales like U/s, with U the mean inlet velocity and s the distance between the inlets, hence confirming the two-dimensional nature of the oscillator-like dynamics. Lastly, the use of sensitivity analysis helps us in identifying the Kelvin-Helmholtz instability, located in the jet's interaction region, as the main candidate for the origin of the oscillations observed in these jet-interaction fluidic devices.